2.5. Electrostatic interactivity

The electrostatic interactivity of the anionic vesicles was evaluated using the change in the zeta potential in presence of Ca^{2+}, pentalysine, and poly-L-lysine (Mw. 15–30 kDa) as an index. A 10 μL aliquot of vesicles (lipid concentration: 2 g/dL) was diluted in 2 mL of 10 mM 2-[4-(2-Hydroxyethyl)-1-piperazinyl] ethanesulfonic acid (HEPES) buffer (pH 7.4, 37 °C) containing 0–3 mM $CaCl_2$ and 17–20 mM NaCl (total 20 mM), or containing varying amounts of pentalysine or poly-L-lysine (Mw. 15–30 kDa) with 20 mM NaCl. The dispersions were incubated for 1 h at 37 °C before mobility measurement of the vesicles was performed by electrophoresis as described in Section 2.4.

2.6. Animal experiments

Animal experiments were conducted under the guidelines recommended by the National Institutes of Health, Animal Use and Care and the protocol was approved by the Steering Committee for Animal Experimentation at Waseda University. Male Wistar rats (250±20 g) were anesthetized with ether. The vesicular dispersion (5 g/dL) was introduced into rats through the tail veins at 1 mL/min (n=5 for each sample). Each rat received 5.6 mL/kg of body weight of vesicle dispersion (lipids: 280 mg/kg of body weight). At 1 or 24 h after injection, the blood was collected and centrifuged to separate the serum (1×10^3 g, 10 min). The collected serum was further ultracentrifuged to remove the vesicles (3×10^5 g, 30 min). The 50% hemolytic unit of complement serum (CH50) was determined in accordance with general procedures for clinical laboratory tests by a commercial company (BML, Japan).

2.7. Statistical methods

The data from the animal experiments are reported as means±standard error of the mean. Statistical analysis was performed using Microsoft Excel for Windows and CH50 values were compared using Student's unpaired t test.

3. Results and discussion

3.1. Samples

Two characteristic acidic lipids used in this study are shown in Fig. 1. SA and PG each have carboxylic acid and phosphoric acid as ionized groups, respectively. Both lipids have a strongly hydrophobic dialkyl structure to fix the ionized groups on vesicle surface. The molecular length indicated by the CPK model showed that the carboxylate anion of SA and the phosphate anion of PG would be located at the surface of PC-vesicles (Fig. 1B). Various amounts of SA and PG were incorporated into the PC/CH membrane (1:1, molar ratio) of the anionic vesicles. The size of vesicles was controlled by extrusion methods (final pore size: 0.2 μm), with final mean diameters of approximately 200 nm (Table 1). The vesicles prepared without acidic lipids or with 1 mol% of acidic lipids tended to be slightly larger (ca 30 nm) than vesicles containing more acidic lipids. This effect of acidic lipids on the size of vesicles could be due to the improved dispersion stability of vesicles and electrostatic repulsion of the anionic surfaces. The vesicles without acidic lipids were observed to precipitate in a day, indicating poor dispersion stability. When the vesicles without acidic lipids contain a small amount of PEG-DSPE to prevent the aggregation of vesicles, the diameter of vesicles without acidic lipids was 202±49 nm. Therefore, we guess that the slightly large diameter of vesicles without acidic lipids or with 1 mol% of acidic lipids would be caused by the high aggregability of vesicles. The low aggregability of vesicles having a large zeta potential due to the electrostatic repulsive interaction between vesicles is an advantage of anionic vesicles as stable dispersions.

Table 1
Diameter of prepared vesicles containing various amounts of acidic lipid

Acidic lipid (mol%)	Mean diameter±SD (nm)	
	SA-vesicles	PG-vesicles
0 (PC-vesicles)	232±60	232±60
1	224±58	230±60
5	193±50	196±58
9	205±40	204±49
15	194±45	199±55
20	198±52	194±64

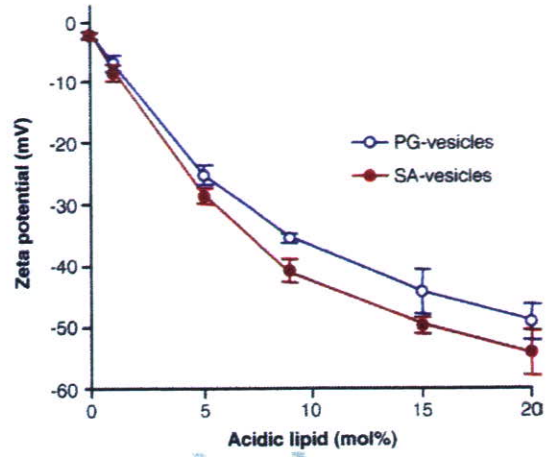

Fig. 2. Zeta potential of vesicles modified with SA (SA-vesicles) and PG (PG-vesicles) as a function of acidic lipid content. Zeta potentials were measured in 10 mM phosphate buffer (pH 7.4, NaCl; 20 mM) at 37 °C.

3.2. Zeta potential of vesicles

The zeta potential is the electrostatic potential at the hydrodynamic slip plane, and is characterized as having an electrical double-layer consisting of the Stern layer and the diffuse layer. Fig. 2 shows the zeta potential of prepared vesicles as a function of acidic lipid content at pH 7.4. Vesicles containing PC/CH (1:1, molar ratio) have an almost neutral surface (zeta potential: −2.22±0.62 mV), indicating that the surface is inactive for electrostatic events. The magnitude of the negative charge on the surface increased with the incorporation of SA or PG, indicating that the ionized groups of SA and PG act to characterize the vesicle surface depending on their content. The zeta potentials of SA-vesicles and PG-vesicles reached −54.2±3.68 mV and −49.0±2.89 mV for acidic lipids of 20 mol%, respectively, with the negative zeta potential of SA-vesicles being relatively higher compared to that of PG-vesicles at any concentration. In theory, the electrostatic potential is dependent upon distance from the membrane surface as well as surface charge density [22]. The slightly extended negative charge of SA from the surface shown in Fig. 1B, would reduce the distance between the change to slip plane, resulting in the higher negative zeta potential of SA-vesicles.

Please cite this article as: K. Sou, E. Tsuchida, Electrostatic interactions and complement activation on the surface of phospholipid vesicle containing acidic lipids: Effect of the structure of acidic groups, Biochim. Biophys. Acta (2008), doi:10.1016/j.bbamem.2008.01.006

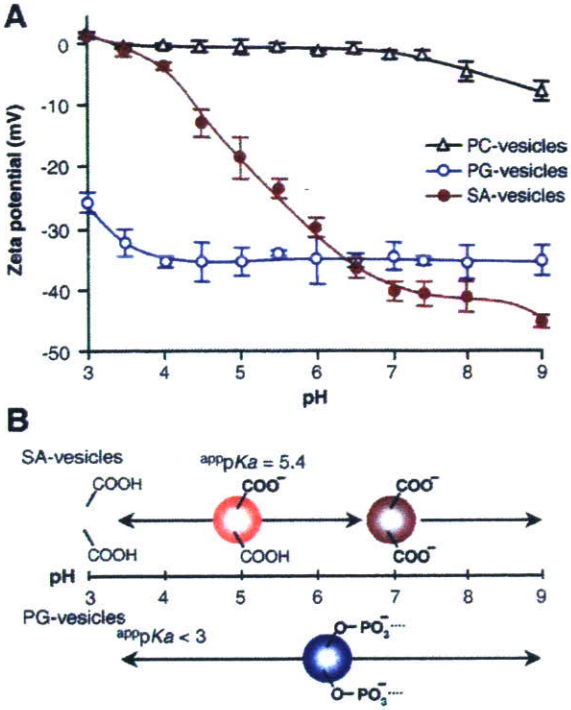

Fig. 3. Ionization state of acidic groups as a function of pH. (A) Zeta potential of vesicles (PC/CH, 1:1, molar ratio) (PC-vesicles), and vesicles containing 9 mol% of SA (SA-vesicles) or PG (PG-vesicles) at various pH. Zeta potentials were measured in 10 mM phosphate buffer (NaCl; 20 mM) at various pH (37 °C). (B) Schematic representation of the ionization state of acidic groups with pH. The apparent pK_as of SA-vesicles and PG-vesicles were calculated to be 5.4 and <3.

This result demonstrated that the capacity of SA as an anionic component of vesicles is equal to acidic phospholipids at pH 7.4.

3.3. Ionization properties of acidic lipids

Stability of the ionization state conferred by acidity is an important characteristic of acidic compounds. We examined the ionization properties of acidic lipids as a function of pH using SA-vesicles and PG-vesicles containing acidic lipids of 9 mol% with zeta potentials of −40.7±2.09 mV and −35.4±0.61 mV (at pH 7.4), respectively. As shown in Fig. 3A, the zeta potential of SA-vesicles varied markedly depending on the environmental pH (pH 3–7). The change in the zeta potential of SA-vesicles is thought to reflect the ionization state of SA, as control vesicles without SA, namely PC-vesicles, maintained almost neutral surfaces irrespective of pH. The relationship between pH and the pK_a of the acid is expressed using the well-known Henderson–Hasselbalch equation as follows:

$$\mathrm{pH} = \mathrm{p}K_a + \log\frac{[-\mathrm{COO}^-]}{[-\mathrm{COOH}]}. \quad (2)$$

When we analyzed the data shown in Fig. 3A using Eq. (2) and the assumption that the zeta potential was linearly correlated with the ionization acid, the pK_a of the carboxyl group of SA was estimated as 5.4 (Fig. 3B). Above pH 7, the zeta potential of SA-vesicles was almost constant, indicating that the carboxyl group of SA would mostly be ionized above pH 7. The zeta potentials of PG-vesicles were almost constant in the range pH 4–9, indicating that the ionized form of the phosphoric acid moiety is stable in this range. The change in the zeta potential observed at a pH lower than pH 4, and its pK_a would be lower than pH 3 [23,24]. Thus, we confirmed that the surface of SA-vesicles and PG-vesicles exhibited the characteristics of a weak acid with SA and a strong acid with PG, respectively, indicating that the individual characteristics of acidic groups are expressed on the surface of vesicles. We also observed that the magnitude of the negative electrostatic charges in SA-vesicles was equal to that observed in PG-vesicles at approximately neutral pH.

3.4. Electrostatic interactivity

Ca^{2+} is found in biological fluids (normally 2–3 mM in plasma) and is known to mediate biological processes by binding to the anionic domains such as those involved in the specific binding of proteins to membranes [25,26]. Acidic phospholipids, such as PG and PS, are also known to bind Ca^{2+} [27–29]. As shown in Fig. 4, the negative charge on anionic vesicles was suppressed by increasing the concentration of Ca^{2+}. When the concentration of Ca^{2+} was increased to 3 mM, the zeta potentials of SA-vesicles and PG-vesicles were −16.4±1.9 mV and −13.8±1.4 mV, respectively. Recently, Hautala et al. reported that vesicles containing phosphatidic acid possess a specifically strong affinity for Ca^{2+}, and that the zeta potential of these vesicles changed from being strongly negative to positive after binding Ca^{2+} [29]. These authors also showed that other acidic phospholipids, including PG, do not exhibit a strong affinity towards becoming cationic. Consequently, one aim of this experiment was to determine whether the binding of Ca^{2+} is a specificity factor between SA-vesicles and PG-vesicles, and also whether the surface of SA-vesicles remained negative in the presence of Ca^{2+}. Our experiment showed that the surface of the SA-vesicles remained

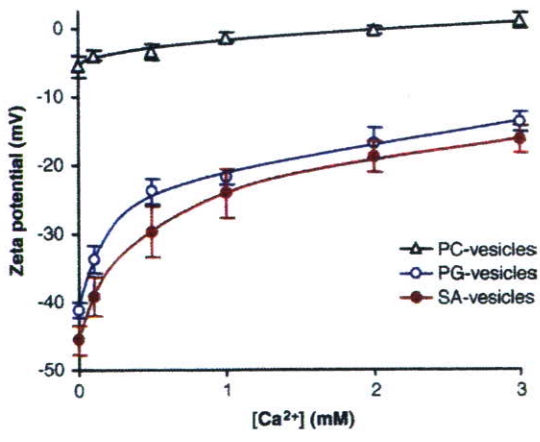

Fig. 4. Change in zeta potential of vesicles as a function of Ca^{2+} concentration. Vesicles were dispersed at 100 μg/mL in 10 mM HEPES buffer (pH 7.4, at 37 °C) containing NaCl and $CaCl_2$ (total: 20 mM). PC-vesicles: PC/ CH (1:1, molar ratio), SA-vesicles: PC/CH/SA (1:1:0.2, molar ratio), and PG-vesicles: PC/CH/PG (1:1:0.2, molar ratio).

Please cite this article as: K. Sou, E. Tsuchida, Electrostatic interactions and complement activation on the surface of phospholipid vesicle containing acidic lipids: Effect of the structure of acidic groups, Biochim. Biophys. Acta (2008), doi:10.1016/j.bbamem.2008.01.006

negative in the presence of Ca^{2+}. In addition, comparisons of SA-vesicles and PG-vesicles also showed that the specificity of binding Ca^{2+} was not observed.

Additional model-based studies of electrostatic interactivity, pentalysine and poly-L-lysine (Mw. 15–30 kDa with a repeating primary lysine amine) were also conducted. Oligomers or polymers of lysine are often used to model basic peptides or macromolecules and their electrostatic interactions on membranes [30,31]. As shown in Fig. 5, the zeta potential is a linear function of the concentration of pentalysine. The lines, which represent the least-squares best fit, have slopes of 9.3 and 7.4 mV per decade for the pentalysine concentrations in SA-vesicles and PG-vesicles. The slope for PC-vesicles was as little as 0.26 mV per decade of pentalysine concentration (data not shown), indicating that the negative charge of acidic lipids mediate the interaction with basic pentalysine. A change in the zeta potential is due to binding of basic peptide [31] and a similar decay slope of the zeta potential would indicate that the binding constant of a basic peptide to SA-vesicles and PG-vesicles was similar. As shown in Fig. 6, the change in the zeta potential of these vesicles due to the interaction with poly-L-lysine increased drastically, changing from a negative to a positive in presence of 1.5–2 μg/mL poly-L-lysine. Conversely, the change in the surface potential of PC-vesicles was negligible, indicating that the acidic lipids mediate the interaction with basic macromolecules. This experiment also demonstrates that the interactivity of SA-vesicles and PG-vesicles to basic macromolecules is equal at pH 7.4, and that within an electrostatic context, SA-vesicles and PG-vesicles interact similarly with basic compounds at physiological pH. It has been shown that electrostatic interactions are involved in the binding of C1q to the surface of anionic vesicles containing acidic phospholipid [6]. In the event that the negative charge on the surface of vesicles is critical for complement activation, both the SA-vesicles and PG-vesicles should be capable of activating the complement system to similar degree. We therefore conducted animal experiments to clarify the issue of complement activation by the anionic electrostatic charge of vesicles.

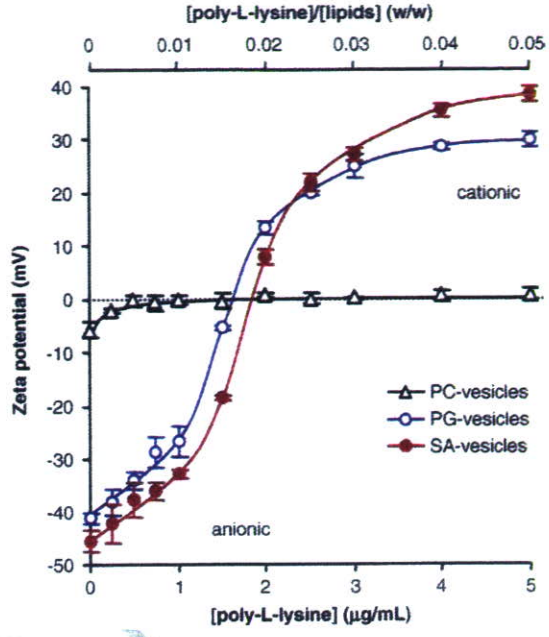

Fig. 6. Change in zeta potential of vesicles as a function of the concentration of basic macromolecule (poly-L-lysine, Mw. 15–30 kDa). Vesicles were dispersed at 100 μg/mL in 10 mM HEPES buffer (pH 7.4, at 37 °C, NaCl, 20 mM) containing various amount of poly-L-lysine. PC-vesicles: PC/CH (1:1, molar ratio), SA-vesicles: PC/CH/SA (1:1:0.2, molar ratio), and PG-vesicles: PC/CH/PG (1:1:0.2, molar ratio).

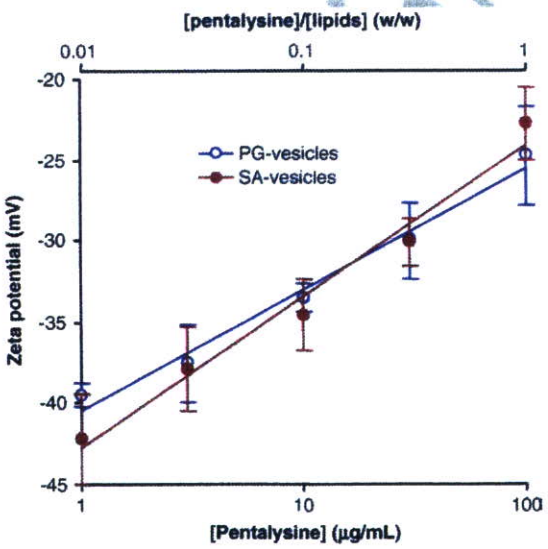

Fig. 5. Change in zeta potential of vesicles as a function of the concentration of basic oligomer (pentalysine). Vesicles were dispersed at 100 μg/mL in 10 mM HEPES buffer (pH 7.4, at 37 °C, NaCl, 20 mM) containing various amount of pentalysine. The lines have slopes of 9.3 and 7.4 mV per decade for the pentalysine concentrations in SA-vesicles and PG-vesicles. SA-vesicles: PC/CH/SA (1:1:0.2, molar ratio) and PG-vesicles: PC/CH/PG (1:1:0.2, molar ratio).

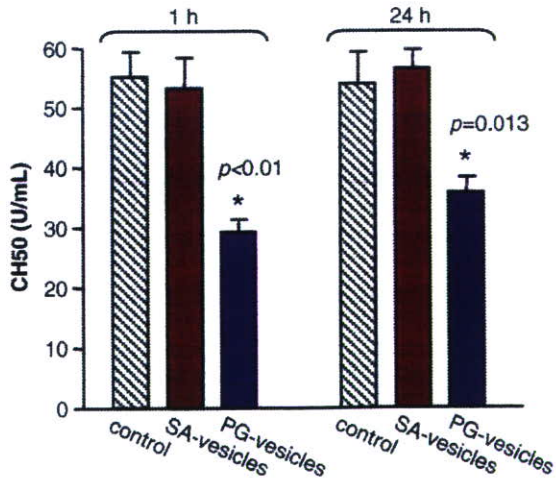

Fig. 7. Comparison of the 50% hemolytic unit of complement (CH50) in rat serum at 1 or 24 h after infusion of saline (control), SA-vesicles, or PG-vesicles. CH50 value for PG-vesicles was significantly lower than that of the control ($p<0.01$ at 1 h, $p=0.013$ at 24 h), indicating the complement consumption in serum after activation. Equal CH50 value for SA-vesicles with the control indicates that SA-vesicles failed to activate complement.

Please cite this article as: K. Sou, E. Tsuchida, Electrostatic interactions and complement activation on the surface of phospholipid vesicle containing acidic lipids: Effect of the structure of acidic groups, Biochim. Biophys. Acta (2008), doi:10.1016/j.bbamem.2008.01.006

3.5. Complement activation

Serum was collected at 1 and 24 h after the infusion of SA-vesicles or PG-vesicles in experimental rats to determine CH50 levels. The control group received saline as a vehicle. The values of CH50 in control rats, and SA-vesicles- and PG-vesicles-administered rats, were 55.1±4.1 U/mL, 53.2±4.8 U/mL, and 29.3±1.6 U/mL at 1 h after infusion of sample, respectively. At 24 h, the values of CH50 in control rats, and SA-vesicles- and PG-vesicles-administered rats, were 54.0±4.7 U/mL, 56.5±3.3 U/mL, and 35.8±2.3 U/mL, respectively (Fig. 7). The lower CH50 levels observed in the PG-vesicles-administered group in comparison with the control group indicate that complement consumption occurred after activation. These findings imply that significant complement activation is induced in rats receiving PG-vesicles compared to the control group ($p<0.01$ at 1 h, $p=0.013$ at 24 h). Complement consumption was not observed in rats administered SA-vesicles.

Since the negative charge and electrostatic interactivity of SA-vesicles were the same as in PG-vesicles (Figs. 2–6), the data obtained from the animal experiments indicates that the negative charge on the anionic vesicle is not a critical factor underlying the activation of complement. The first step in the activation of the classical complement pathway involves the binding of an activator to C1q, resulting in the activation of serine proteases C1r and C1s. It has been suggested that the negative charge of an activator such as PG-vesicles is involved in some way with the binding of the activator to C1q [1–8]. Assuming that the electrostatic interaction is non-specific, SA-vesicles should interact with C1q electrostatically. Since the action of complement proteases, which follows the binding of the activator to the C1q, is known to be highly specific [32,33], it seems likely that complement activation on anionic surface is limited to an activation step rather than a binding step. Such specific activation of complement by the anionic vesicles in the present study may be involved in the physiological regulation of complement activation on anionic biomembranes.

4. Conclusions

The carboxylic acid of SA and phosphoric acid of PG have equal capacity as anionic components of vesicles at neutral pH. The results presented in this investigation demonstrated that the negative electrostatic charge of anionic vesicles is not a critical factor in the activation of complement. Rather, the induction of complement activation by anionic vesicles is dependent on the structure of acidic lipids. This finding may facilitate development and various biological applications of anionic vesicles.

Acknowledgements

This work was partly supported by Health Sciences Research Grants (Research on Regulatory Science); the Ministry of Health, Labour and Welfare, Japan, and the Ministry of Education, Science, Sports and Culture, Grant-in-Aid for Scientific Research (B), 17300162. The authors gratefully acknowledge Dr. K. Kobayashi and Dr. H Horinouchi (Keio University) for their support in the animal experiments, Dr. M. Suematsu (Keio University) for an important suggestion on bioactivity of anionic vesicles, and Dr. S. Takeoka and Dr. H. Sakai (Waseda University) for advice and discussions related to this research.

References

[1] H.C. Loughrey, M.B. Bally, L.M. Reinish, P.R. Cullis, The binding of phosphatidylglycerol liposomes to rat platelets is mediated by complement, Thromb. Haemost. 64 (1990) 172–176.
[2] A. Chonn, P.R. Cullis, D.V. Devine, The role of surface charge in the activation of the classical and alternative pathways of complement by liposomes, J. Immunol. 146 (1991) 4234–4241.
[3] J. Szebeni, The interaction of liposomes with the complement system, Crit. Rev. Ther. Drug Carr. Syst. 15 (1998) 57–88.
[4] S.M. Moghimi, I. Hamad, T.L. Andresen, K. Jorgensen, J. Szebeni, Methylation of the phosphate oxygen moiety of phospholipid-methoxy (polyethylene glycol) conjugate prevents PEGylated liposome-mediated complement activation and anaphylatoxin production, FASEB J. 20 (2006) 2591–2593.
[5] A.J. Bradley, D.E. Brooks, R. Norris-Jones, D.V. Devine, C1q binding to liposomes is surface charge dependent and is inhibited by peptides consisting of residues 14–26 of the human C1qA chain in a sequence independent manner, Biochim. Biophys. Acta 1418 (1999) 19–30.
[6] A.J. Bradley, E. Maurer-Spurej, D.E. Brooks, D.V. Devine, Unusual electrostatic effects on binding of C1q to anionic liposomes: role of anionic phospholipid domains and their line tension, Biochemistry 38 (1999) 8112.
[7] H. Jiang, B. Cooper, F.A. Robey, H. Gewurz, DNA binds and activates complement via residues 14–26 of the human C1q A chain, J. Biol. Chem. 267 (1992) 25597–25601.
[8] H. Jiang, D. Burdick, C.G. Glabe, C.W. Cotman, A.J. Tenner, beta-Amyloid activates complement by binding to a specific region of the collagen-like domain of the C1q A chain, J. Immunol. 152 (1994) 5050–5059.
[9] A.J. Bradley, D.V. Devine, S.M. Ansell, J. Janzen, D.E. Brooks, Inhibition of liposome-induced complement activation by incorporated poly(ethylene glycol)-lipids, Arch. Biochem. Biophys. 357 (1998) 185–194.
[10] E. Tsuchida (Ed.), Substitute: Present and Future Perspective, Elsevier Science, Amsterdam, 1998.
[11] S. Takeoka, T. Ohgushi, K. Terase, T. Ohmori, E. Tsuchida, Layer-controlled hemoglobin vesicles by interaction of hemoglobin with a phospholipid assembly, Langmuir 12 (1996) 1755–1759.
[12] H. Sakai, K. Hamada, S. Takeoka, H. Nishide, E. Tsuchida, Physical properties of hemoglobin vesicles as red cell substitutes, Biotechnol Prog. 12 (1996) 119–125.
[13] K. Sou, Y. Naito, T. Endo, S. Takeoka, E. Tsuchida, Effective encapsulation of proteins into size-controlled phospholipid vesicles using freeze-thawing and extrusion, Biotechnol Prog. 19 (2003) 1547–1552.
[14] H. Sakai, H. Horinouchi, M. Yamamoto, E. Ikeda, S. Takeoka, M. Takaori, E. Tsuchida, K. Kobayashi, Acute 40 percent exchange-transfusion with hemoglobin-vesicles (HbV) suspended in recombinant human serum albumin solution: degradation of HbV and erythropoiesis in a rat spleen for 2 weeks, Transfusion 46 (2006) 339–347.
[15] H. Saka i, Y. Masada, H. Horinouchi, E. Ikada, K. Sou, S. Takeoka, M. Suematsu, M. Takaori, K. Kobayashi, E. Tsuchida, Physiological capacity of the reticuloendothelial system for the degradation of hemoglobin vesicles (artificial oxygen carriers) after massive intravenous doses by daily repeated infusions for 14 days, J. Pharmacol. Exp. Ther. 311 (2004) 874–884.
[16] K. Sou, R. Klipper, B. Goins, E. Tsuchida, W.T. Phillips, Circulation kinetics and organ distribution of Hb-vesicles developed as a red blood cell substitute, J. Pharmacol. Exp. Ther. 312 (2005) 702–709.
[17] H. Abe, M. Fujihara, H. Azuma, H. Ikeda, K. Ikebuchi, S. Takeoka, E. Tsuchida, H. Harashima, Interaction of hemoglobin vesicles, a cellular-type artificial oxygen carrier, with human plasma: effects on coagulation, kallikrein-kinin, and complement systems, Artif. Cells Blood Substit. Biotechnol. 34 (2006) 1–10.

Please cite this article as: K. Sou, E. Tsuchida, Electrostatic interactions and complement activation on the surface of phospholipid vesicle containing acidic lipids: Effect of the structure of acidic groups, Biochim. Biophys. Acta (2008), doi:10.1016/j.bbamem.2008.01.006

[18] H. Abe, H. Azuma, M. Yamaguchi, M. Fujihara, H. Ikeda, H. Sakai, S. Takeoka, E. Tsuchida, Effects of hemoglobin vesicles, a liposomal artificial oxygen carrier, on hematological responses, complement and anaphylactic reactions in rats, Artif. Cells Blood Substit. Biotechnol. 35 (2007) 157–172.
[19] K. Sou, B. Goins, S. Takeoka, E. Tsuchida, W.T. Phillips, Selective uptake of surface-modified phospholipid vesicles by bone marrow macrophages in vivo, Biomaterials 28 (2007) 2655–2666.
[20] K. Sou, T. Endo, S. Takeoka, E. Tsuchida, Poly(ethylene glycol)-modification of the phospholipid vesicles by using the spontaneous incorporation of poly (ethylene glycol)-lipid into the vesicles, Bioconjug. Chem. 11 (2000) 372–379.
[21] H. Saka i, S. Hisamoto, I. Fukutomi, K. Sou, S. Takeoka, E. Tsuchida, Detection of lipopolysaccharide in hemoglobin-vesicles by Limulus amebocyte lysate test with kinetic-turbidimetric gel clotting analysis and pretreatment of surfactant, J. Pharm. Sci. 93 (2004) 310–321.
[22] S. McLaughlin, The electrostatic properties of membranes, Annu. Rev. Biophys. Biophys. Chem. 18 (1989) 113–136.
[23] A. Watts, K. Harlos, W. Maschke, D. Marsh, Control of the structure and fluidity of phosphatidylglycerol bilayers by pH titration, Biochim. Biophys. Acta 510 (1978) 63–74.
[24] J.F. Tocanne, J. Teissié, Ionization of phospholipids and phospholipid-supported interfacial lateral diffusion of protons in membrane model systems, Biochim. Biophys. Acta 1031 (1990) 111–142.
[25] J. Rizo, T.C. Sudhof, C2-domains, structure and function of a universal Ca^{2+}-binding domain, J. Biol. Chem. 273 (1998) 15879–15882.
[26] J.E. Murphy, D. Tacon, P.R. Tedbury, J.M. Hadden, S. Knowling, T. Sawamura, M. Peckham, S.E. Phillips, J.H. Walker, S. Ponnambalam, LOX-1 scavenger receptor mediates calcium-dependent recognition of phosphatidylserine and apoptotic cells, Biochem. J. 393 (2006) 107–115.
[27] A. Lau, A. McLaughlin, S. McLaughlin, The adsorption of divalent cations to phosphatidylglycerol bilayer membranes, Biochim. Biophys. Acta 645 (1981) 279–292.
[28] C.G. Sinn, M. Antonietti, R. Dimova, Binding of calcium to phosphatidylcholine-phosphatidylserine membranes, Colloids and Surfaces A: Physicochem. Eng. Aspects 282–283 (2006) 410–419.
[29] J.T. Hautala, M.L. Riekkola, S.K. Wiedmer, Anionic phospholipid coatings in capillary electrochromatography. Binding of Ca^{2+} to phospholipid phosphate group, J. Chromatogr. A 1150 (2007) 339–347.
[30] D. Volodkin, V. Ball, P. Schaaf, J.C. Voegel, H. Mohwald, Complexation of phosphocholine liposomes with polylysine, Stabilization by surface coverage versus aggregation, Biochim. Biophys. Acta 1768 (2007) 280–290.
[31] D. Murray, A. Arbuzova, G. Hangyas-Mihályné, A. Gambhir, N. Ben-Tal, B. Honig, S. MaLaughlin, Electrostatic properties of membranes containing acidic lipids and adsorbed basic peptides: theory and experiment, Biophys. J. 77 (1999) 3176–3188.
[32] G.J. Arlaud, C. Gaboriaud, N.M. Thielens, M. Budayova-Spano, V. Rossi, J.C. Fontecilla-Camps, Structural biology of the C1 complex of complement unveils the mechanisms of its activation and proteolytic activity, Mol. Immunol. 39 (2002) 383–394.
[33] G. O'Brien, N.S. Quinsey, J.C. Whisstock, R.N. Pike, Importance of the prime subsites of the C1s protease of the classical complement pathway for recognition of substrates, Biochemistry 42 (2003) 14939–14945.

Please cite this article as: K. Sou, E. Tsuchida, Electrostatic interactions and complement activation on the surface of phospholipid vesicle containing acidic lipids: Effect of the structure of acidic groups, Biochim. Biophys. Acta (2008), doi:10.1016/j.bbamem.2008.01.006

Available online at www.sciencedirect.com
ScienceDirect
International Journal of Pharmaceutics 352 (2008) 287–293
INTERNATIONAL JOURNAL OF PHARMACEUTICS
www.elsevier.com/locate/ijpharm

Pharmaceutical Nanotechnology

Loading of curcumin into macrophages using lipid-based nanoparticles

Keitaro Sou, Shunsuke Inenaga, Shinji Takeoka, Eishun Tsuchida*

Advanced Research Institute for Science and Engineering, Waseda University, Tokyo 169-8555, Japan

Received 3 July 2007; received in revised form 28 August 2007; accepted 21 October 2007
Available online 1 November 2007

Abstract

Curcumin (1,7-bis(4-hydroxy-3-methoxyphenyl)-1,6-heptadiene-3,5-dione, Cm) is a natural compound which possesses antioxidant, anti-inflammatory and anti-tumor ability. Here, phospholipid vesicles or lipid-nanospheres embedding Cm (CmVe or CmLn) were formulated to deliver Cm into tissue macrophages through intravenous injection. Cm could be solubilized in hydrophobic regions of these particles to form nanoparticle dispersions, and these formulations showed ability to scavenge reactive oxygen species as antioxidants in dispersions. At 6 h after intravenous injection in rats via the tail vein (2 mg Cm/kg bw), confocal microscopic observations of tissue sections showed that Cm was massively distributed in cells assumed as macrophages into the bone marrow and spleen. Taken together, these results indicate that the lipid-based nanoparticulates provide improved intravenous delivery of Cm to tissues macrophages, specifically bone marrow and splenic macrophages in present formulation, which has therapeutic potential as an antioxidant and anti-inflammatory.

Keywords: Nanoparticles; Liposomes; Bone marrow; Macrophage; Antioxidant; Drug delivery

1. Introduction

Because of the significant phagocytic ability of the mononuclear phagocyte system (MPS) to nanoparticles *in vivo*, drug delivery which targets macrophages can be reasonably achieved by using nanoparticles. Recent studies indicated that macrophages relate with various diseases associated with inflammation and the macrophage targeting may open new therapeutic approaches for controlling the diseases (Chellat et al., 2005; Zeisberger et al., 2006; Schmid and Varner, 2007).

Curcumin (1,7-bis(4-hydroxy-3-methoxyphenyl)-1,6-heptadiene-3,5-dione, Cm) (Fig. 1) is a natural compound isolated from the root of *Curcuma longa* that has been shown to exhibit antioxidant, anti-inflammatory and anti-tumor abilities (Kunchandy and Rao, 1990; Singh and Aggarwal, 1995; Kuo et al., 1996; Shishodia et al., 2005; Sharma et al., 2005). Cm has been demonstrated to have scavenger ability against reactive oxygen species (ROS), such as superoxide anion ($O_2^{\bullet -}$), hydrogen peroxide (H_2O_2) and nitric oxide (NO), both *in vitro* and *in vivo* (Kunchandy and Rao, 1990). In addition, it has been reported to be a potent inducer of heme oxygenase-1 in vascular endothelial cells (Motterlini et al., 2000). These properties contribute to the protection of cells and tissue from oxidative stress. Further, anti-inflammatory ability of Cm is induced by the suppression of nuclear factor-kappa B (NF-κB) activation, which results in the inhibition of synthesis of inducible nitric oxide synthase (iNOS) in macrophages (Pan et al., 2000). Thus, macrophages can be a therapeutic targeted cellular component for Cm.

Oral Cm administration as a cancer therapy in phase I clinical studies in humans produced minimal side effects (Cheng et al., 2001; Sharma et al., 2004). However, the clinical pharmacokinetics studies revealed maximum Cm plasma levels in the range of only 1.8–11 nM in patients, even for oral administration of several grams of Cm per day. Thus, the current conclusion on Cm is that it has poor bioavailability when orally administered. This unsatisfactory pharmacokinetics of oral administration is not restricted to Cm, but is also observed for various lipophilic drug candidates.

A promising approach to developing improved delivery systems lipophilic drugs employs lipid-based carriers such as

* Corresponding author. Tel.: +813 5286 3120; fax: +813 3205 4740.
E-mail addresses: ksou@waseda.jp (K. Sou), eishun@waseda.jp (E. Tsuchida).

0378-5173/$ – see front matter © 2007 Elsevier B.V. All rights reserved.
doi:10.1016/j.ijpharm.2007.10.033

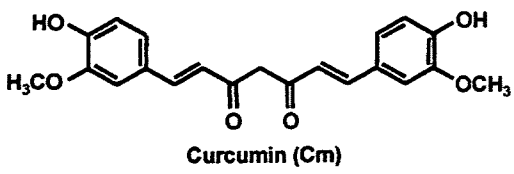

Fig. 1. Structure of curcumin. This compound is insoluble in water because of strong hydrophobicity of diketo moiety.

micelles, vesicles (liposomes), and nano- or microspheres, which can solubilize lipophilic drugs in self-assembling processes. Cm is known to interact with phospholipids or surfactants to solubilize in aqueous dispersions (Began et al., 1999; Tønnesen, 2002; Bruzell et al., 2005). Recently, some investigators have advanced this research to incorporate complexes of Cm with phospholipids in drug delivery systems (Li et al., 2005; Kunwar et al., 2006; Maiti et al., 2007). In immunohistochemical studies, Li et al. observed antiangiogenesis effect following intravenous injection of Cm-liposomes, which suppressed pancreatic carcinoma growth in murine xenograft models (Li et al., 2005). More recently, Maiti et al. reported that intraperitoneal injection of Cm–phospholipid complex has better hepatoprotective activity, owe to its superior antioxidant property, than free Cm (Maiti et al., 2007). These reports indicated that the therapeutic potential of Cm would be enhanced by the development of efficient drug delivery system.

Recently, we found that surface modification of vesicles with L-glutamic acid, *N*-(3-carboxy-1-oxopropyl)-, 1,5-dihexadecyl ester (SA) and poly(ethylene glycol) (PEG)-lipid increases the distribution of vesicles into bone marrow macrophage when injected in small doses (Sou et al., 2007). This finding is applied for the intravenous delivery of Cm to tissue macrophages in this study. Here, nano-sized vesicles containing Cm (CmVe) and lipid-nanospheres (CmLn) were prepared and characterized. Furthermore, distribution of Cm in organs after intravenous injection in rats was observed. We show that these nanoparticle systems would be available to deliver Cm to tissues macrophages, specifically bone marrow and splenic macrophages in present system.

2. Materials and methods

2.1. Materials

1,2-Dimyristoyl-*sn*-glycero-3-phosphocholine (DMPC) and L-glutamic acid, *N*-(3-carboxy-1-oxopropyl)-, 1,5-dihexadecyl ester (SA) were purchased from Nippon Fine Chemical Co. Ltd. (Osaka, Japan); 1,2-distearoyl-*sn*-glycero-3-phosphoethanolamine-*N*-[monomethoxy poly(ethylene glycol) (5000)] (PEG-DSPE) was purchased from NOF Co. (Tokyo, Japan). Soybean oil was purchased from Kanto Chemical Co. (Tokyo, Japan). Curcumin (Cm) was purchased from SIGMA (St. Louis, MO, USA). 8-Amino-5-chloro-7-phenylpyrid[3,4-*d*]pyridazine-1,4-(2H,3H) dione sodium salt (L-012), hypoxanthine, xanthine oxidase, and superoxide dismutase (SOD, 3400 U/mg), were purchased from Wako Pure Chemical Industries (Tokyo, Japan).

2.2. Preparation of CmVe

Lipid powder of DMPC/SA/PEG-DSPE (10/1/0.06, molar ratio) and Cm were dissolved in the mixed solvent system of *t*-butyl alcohol and benzene (1/1, v/v) and then lyophilized to obtain mixed lipid powder containing Cm. The lyophilized powder was hydrated in physiological saline at 70 mg mL^{-1} for 30 min under stirring by a vortex mixer. The dispersion was subjected to extrusion (final pore size of the filter: 0.2 μm, Isopore®, Millipore, Tokyo, Japan) and finally filtered through sterilized filters (pore size: 0.2 μm Dismic, Toyo Roshi, Tokyo, Japan) to obtain fine-sized Cm-vesicles (CmVe). Sample preparation for animal experiment was performed under sterilized conditions.

2.3. Preparation of CmLn

To prepare the Cm lipid-nanosphere formulation (CmLn), Cm was dissolved in soybean oil (10 mg mL^{-1}) at 150 °C, and then mixed with lipid powder comprising DMPC/SA/PEG-DSPE (10/1/0.06, molar ratio) dissolved in soybean oil (280 mg mL^{-1}) at 60 °C. This mixed solution was introduced into 2.5% glycerin solution under vigorously stirring with a wing stirrer (1200 rpm) and continuously stirred for 30 min to obtain crude lipid-microsphere dispersion. The dispersion was subjected to extrusion to control the size of the lipid-nanosphere (final pore size of the filter: 0.2 μm, Isopore®, Millipore, Tokyo, Japan) and finally passed through sterilized filters (pore size: 0.2 μm Dismic, Toyo Roshi, Tokyo, Japan) to obtain CmLn. Sample preparation for animal experiment was performed under sterilized conditions.

2.4. Characterization of CmVe and CmLn

The concentration of Cm in CmVe and CmLn was determined from calibration curves of absorbance at 420 nm prepared in ethanol, and the concentration of phospholipid was determined using a phospholipid assay kit (Phospholipid C Test Wako, Wako Pure Chemical, Tokyo Japan). The diameter of the resulting CmVe and CmLn was determined with a COULTER submicron particle analyzer (N4SD, Coulter, Hialeah, FL), and represented as an average diameter ± standard deviation (S.D.). The zeta(ζ)-potential was determined with a Zeta-Sizer Nano ZS (Malvern, MA, USA). Florescence imaging was carried out with excitation at 488 nm on a confocal scanning microscope (Olympus IX70, Tokyo, Japan) equipped with an ArKr ion laser system (Yokogawa) and recorded with image analysis software (IPLab version 3.5 for Macintosh, Scanalytics, Inc., VA, USA). Transmission electron microscopy (TEM) was carried out using a negative staining technique. Briefly, equivolumes of the sample and 2% phosphotungstic acid solution were mixed, and then a drop of mixed solution was allowed to settle on a carbon-coated copper grid for 1 min. Excess sample was removed by filter paper, dried in a desiccator, and visualized using a JEOL JEM-1011/100 kV (JEOL, Tokyo Japan).

2.5. Chemiluminescence assay

ROS scavenge ability of CmVe was evaluated by the generation of $O_2^{\bullet -}$ in a hypoxanthine and xanthine oxidase system. L-012 (50 μM) was used for chemiluminescence probe to detect $O_2^{\bullet -}$ according to Nishinaka et al. (1993). Xanthine oxidase, L-012, and CmVe were mixed together in test tube and $O_2^{\bullet -}$ generation was started by the addition of hypoxanthine. The final concentrations of regents were fixed at hypoxanthine, 0.5 mM; xanthine oxidase, 25 mU/mL; and L-120, 50 μM; CmVe was supplied in the concentration range 1–100 μM. Chemiluminescence was counted for 3 min after addition of hypoxanthine using an AccuFLEX Lumi400 from ALOKA (Tokyo, Japan). Ve, having the same lipid concentration with CmVe, was tested with the same procedure to determine the effect of lipid components. In addition, SOD, which is a popular $O_2^{\bullet -}$ scavenger, was tested with the same procedure to serve as a reference for the $O_2^{\bullet -}$ scavenging ability.

2.6. Animal experiments

Animal experiments were performed under the regulations for Animal Experimentation at Waseda University and were approved by the Steering Committee for Animal Experimentation at Waseda University. Male Wister rats (200–218 g) were anesthetized with 2% isoflurane (VedCo, St Joseph, MO, USA) in 100% oxygen gas. Samples were injected into the tail vein at 1 mL/min. Each rat received a total dose of Cm: 2 mg/kg as dispersion of CmVe or CmLn ($n=5$). The blood sample was collected just before injection, and various time after injection to monitor the circulation level of blood cells. At 6 h after injection, the animals were scarified to collect bone marrow, liver, and spleen. The organs were fixed in 10% formaldehyde, sectioned, fixed on glass slides with 2% agar solution, and observed under a confocal scanning microscope (Olympus IX-70).

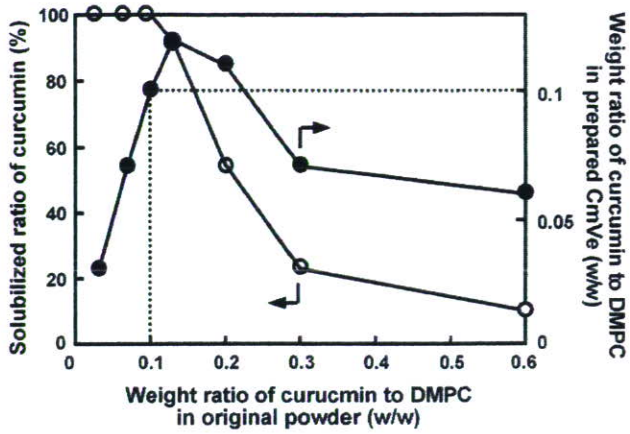

Fig. 2. Solubilization capacity of DMPC-vesicles for curcumin.

3. Results

3.1. Preparation and characterization of CmVe

All DMPC, SA, PEG-DSPE, and Cm compounds were successfully dissolved in mixed solvent of *t*-butyl alcohol and benzene (1/1, volume ratio) and the lyophilized powder was employed for the preparation of vesicles. Initially, we applied various amounts of Cm in order to determine the maximum capacity of vesicles to stably immobilize the Cm. As shown in Fig. 2, when the weight ratio of Cm to DMPC was below 0.1, vesicles could completely solubilize the Cm in dispersion of vesicles. When the weight ratio of employed Cm in the origi-

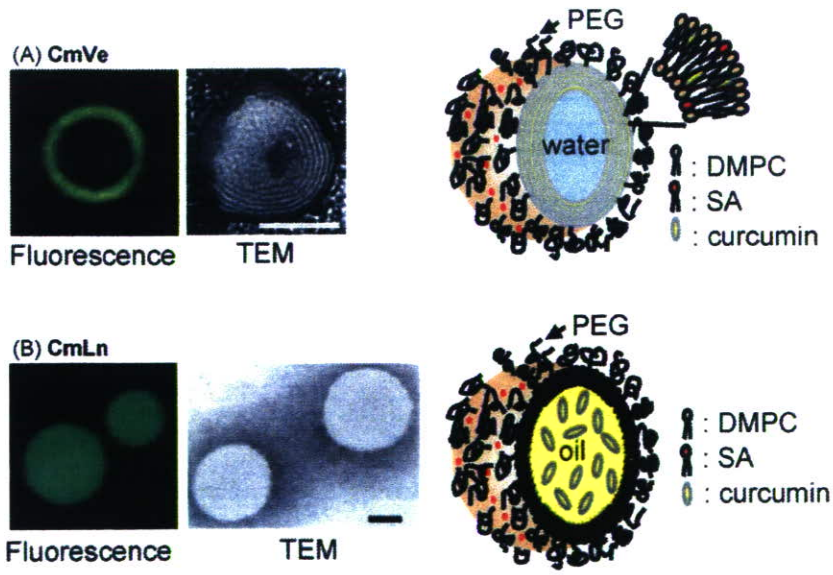

Fig. 3. Structural characterization of (A) DMPC-vesicles comprising curcumin (CmVe) and (B) lipid-nanosphere comprising curcumin (CmLn). Confocal scanning microscopic images (left) and transmission electron micrographs (TEM) (right) of CmVe and CmLn. Confocal scanning microscopic images were taken before extrusion to submicron size to enable observation of the structure within resolution of a confocal microscope. These images indicate the localization of Cm in vesicles and lipid-sphere with diameter of ca. 10 μm. Bars in TEM represent 100 nm. Illustrations are estimated structures of CmVe and CmLn.

Table 1
Diameter and ζ-potential of CmVe and CmLn with and without SA

Particle type	Composition of lipids (molar ratio)	Diameter (nm)	ζ-potential[a] (mV)
CmVe	DMPC/PEG-DSPE (10/0.06)	193 ± 75	−1.99 ± 1.86
	DMPC/SA/PEG-DSPE (10/1/0.06)	187 ± 53	−21.1 ± 1.88
CmLn	DMPC/PEG-DSPE (10/0.06)	219 ± 95	0.018 ± 1.95
	DMPC/SA/PEG-DSPE (10/1/0.06)	217 ± 93	−19.8 ± 0.28

[a] ζ-potential was measured in 10 mM phosphate buffer solution (pH 7.4, NaCl 20 mM).

nal powder was increased above 0.1, an excess fraction of Cm formed an orange solid in dispersion medium during hydration. To control the size of vesicles resulting in the decreasing of solubilized ratio of Cm, the solid Cm was filtrated out in the subsequent extrusion procedure. Therefore, we determined that the capacity of the present vesicles to stably solubilize Cm was 0.1 in weight ratio of Cm to DMPC, a value which is equivalent to 16 mol% Cm in the DMPC membrane. Thus, we determined the stable formulation of vesicles solubilizing Cm in their bilayer membrane to be DMPC/SA/PEG-DSPE/Cm (10/1/0.06/1.9, molar ratio), which is applied for the following experiments as CmVe. We confirmed that 97% of Cm was present in CmVe fraction separated by ultracentrifugation, indicating that little Cm was isolated from Ve in prepared dispersion.

Confocal scanning microscopic observation indicated that the Cm was located in the membrane of vesicles, but not in the inner aqueous phase, while TEM observation showed that the CmVe have an origolamellar structure, which is typically comprised of three to six layers. One representative vesicle is shown in Fig. 3A. The ζ-potential of CmVe was determined to be −21.1 ± 1.88 mV at pH 7.4 and its diameter was 187 ± 53 nm (Table 1). This data showed that the CmVe is a nano-sized anionic particle. The ζ-potential of vesicle prepared without SA was −1.99 ± 1.86 mV, indicating that the incorporation of SA results in an anionic surface. Based on these results, we estimated the structure of CmVe as illustrated in Fig. 3A, where PEG and SA express their physicochemical characters on the surface of CmVe, and Cm locates in the multilayer bilayer membrane. Spectroscopic data further indicate that the location of Cm is in the bilayer membrane. As shown in Fig. 4A, the spectra of CmVe dispersion showed a peak with three compartments. The λ_{max} was observed at 401 nm at 10 °C, where the dispersion was orange rather than yellow. With increasing temperature, the peak at 401 nm decreased and the peak at 420 nm increased to where the color of dispersion changed to yellow. Plotting the absorbance at 420 nm by temperature showed that the absorbance of 420 nm was critically increased between 20 and 30 °C (Fig. 4B). This range corresponded to the gel–liquid crystalline phase transition temperature of DMPC (23 °C) (Pownall et al., 1977), suggesting that the molecular state of Cm is influenced by the phase state of the bilayer membrane. This observation also supported by the fact that Cm is located in the bilayer membrane.

3.2. Preparation and characterization of CmLn

Regarding the preparation of CmLn, the solubility of the Cm in soybean oil was limited to the maximum solubilization of Cm, which has a solubility of approximately 10 mg mL^{-1} at preparation condition (around 25 °C). The same lipid formulation with CmVe [DMPC/SA/PEG-DSPE (10/1/0.06, molar ratio)] was applied for CmLn. The soybean oil solution was injected into 2.5% glycerin solution under stirring. Subsequently, the dispersion was passed through a membrane filter to control the size of CmLn. The incorporation of SA contributed to the anionic surface of CmLn (ζ-potential: −19.8 mV) indicating that the anionic head group of SA is located on the surface of the CmLn

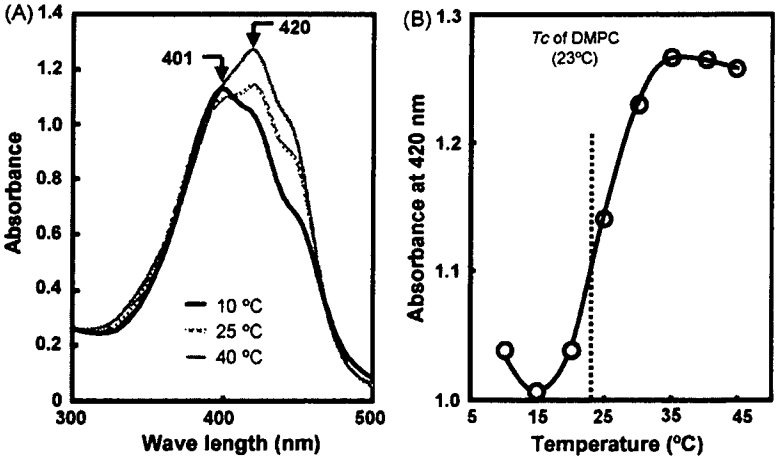

Fig. 4. Spectral property of CmVe dispersion with temperature. (A) Raw spectra at 10, 25, and 40 °C. (B) Absorbance at 420 nm plotted according to temperature. Absorbance of Cm critically changes in range of the gel–liquid crystalline phase transition temperature (T_c, 23 °C) of DMPC membrane, indicating that Cm is embedded in membrane.

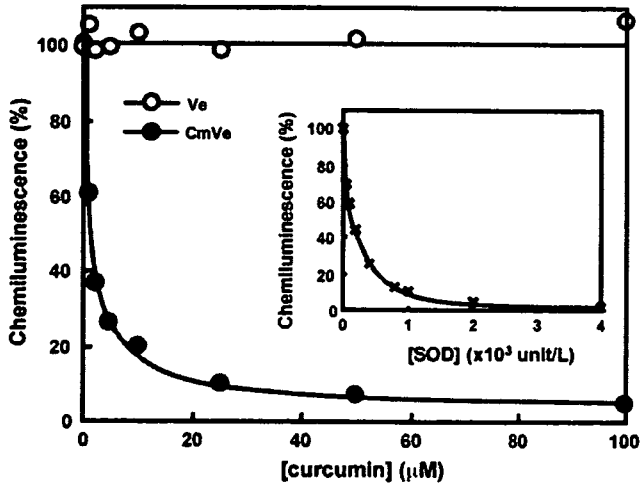

Fig. 5. Scavenging superoxide anion ($O_2^{\bullet -}$) by CmVe as a function of concentration of Cm. $O_2^{\bullet -}$ was produced by hypoxanthine (0.5 mM) and xanthine oxidase (25 mU/mL) system and detected by a chemiluminescence probe L-120 (50 μM). Vesicles without Cm (Ve) are being use as a control. Small panel shows the comparable experiment with SOD.

(Table 1). Confocal scanning microscopic observation indicated that the Cm was located inside the oil phase of Lm, while TEM observation indicated a spherical shape without an inner aqueous phase (Fig. 3B). Based on dynamic light scattering measurement, the diameter of CmLn was determined to be 217 ± 93 nm in dispersion state (Table 1).

3.3. ROS scavenge ability

As shown in Fig. 5, depending on the concentration of Cm, CmVe showed the ability to scavenge generated $O_2^{\bullet -}$ from hypoxanthine and xanthine oxidase system. Based on these data, we determined that the concentration of CmVe required to reduce 50% of chemiluminescence of L-012 by $O_2^{\bullet -}$ was 1.8, and 25 μM is required to reduce 90% of chemiluminescence of L-012 by $O_2^{\bullet -}$, as summarized in Table 2. As comparative index of $O_2^{\bullet -}$ scavenging ability, SOD which ability was defined as unit, was applied in the same $O_2^{\bullet -}$ generation system. As shown in the small panel in Fig. 5 and in Table 2, 160 units/L SOD reduced 50% of chemiluminescence of L-012, and 1050 units/L SOD reduced 90% of chemiluminescence of L-012. Thus, we roughly estimated that the $O_2^{\bullet -}$ scavenger ability in 1.8–25 μmol range of Cm in present formulation of CmVe was comparable to the 160–1050 range of SOD units. DMPC vesicles that consisted of saturated phospholipids and saturated SA were not reactive to $O_2^{\bullet -}$. These data indicate that the present nanoparticulate formulations potentially have ROS scavenger ability.

Table 2
Scavenger ability of CmVe or vesicles without Cm (Ve) to superoxide anion ($O_2^{\bullet -}$) generated from hypoxanthine and xanthine oxidase system

Scavengers	IC_{50}[a]	IC_{90}[a]
CmVe	1.8 μM	25 μM
Ve	na	na
SOD	160 units/L	1050 units/L

[a] IC_{50} and IC_{90} are concentration of Cm to scavenge 50 and 90% of $O_2^{\bullet -}$ (na = not active).

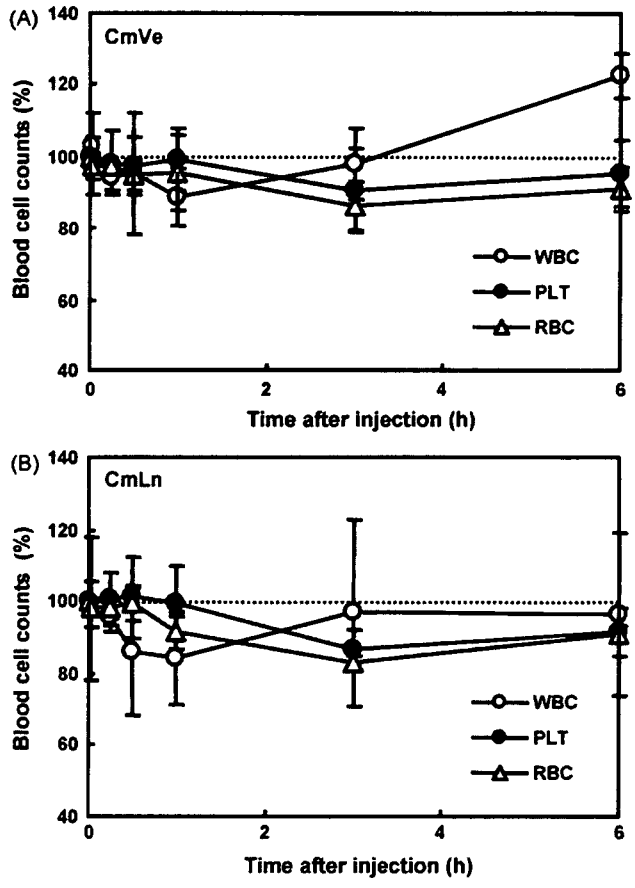

Fig. 6. Profiles of blood cell counts after intravenous infusion of (A) CmVe dispersion or (B) CmLn dispersion in rats. Each rat received 2 mg Cm/kg bw. Percentages are blood cell counts before injection of sample. WBC: white blood cells, PLT: platelets, RBC: Red blood cells.

3.4. Intravenous delivery and distribution in organs

Prepared CmVe or CmLn with SA were intravenously injected in rats to monitor the injection response of blood cells and observe organ distribution. All rats ($n = 5$) received CmVe or CmLn were survived for 6 h after injection. As shown in Fig. 6, no acute response to injection of these formulations was observed in circulating blood cells. In rats receiving CmVe or CmLn, white blood cells (WBC) tended to gradually decrease to 89 ± 8 or 84 ± 13% until 1 h, and then returned to baseline levels. Upper recovery to baseline levels was observed in CmVe at 6 h, but was not observed in CmLn. As for red blood cells (RBC) and platelets (PLT), the circulating level tended to decrease in a similar manner until 3 h, and then returned to baseline. At 6 h, bone marrow, liver, and spleen samples were collected for observation of the distribution of Cm in these tissues. As shown in Fig. 7, confocal scanning microscopy indicated that the Cm emitting yellow fluorescence was located in these tissues. This observation indicated intravenous injection of Cm using present lipid-based nanoparticles could facilitate the delivery of Cm into macrophages especially in bone marrow and spleen.

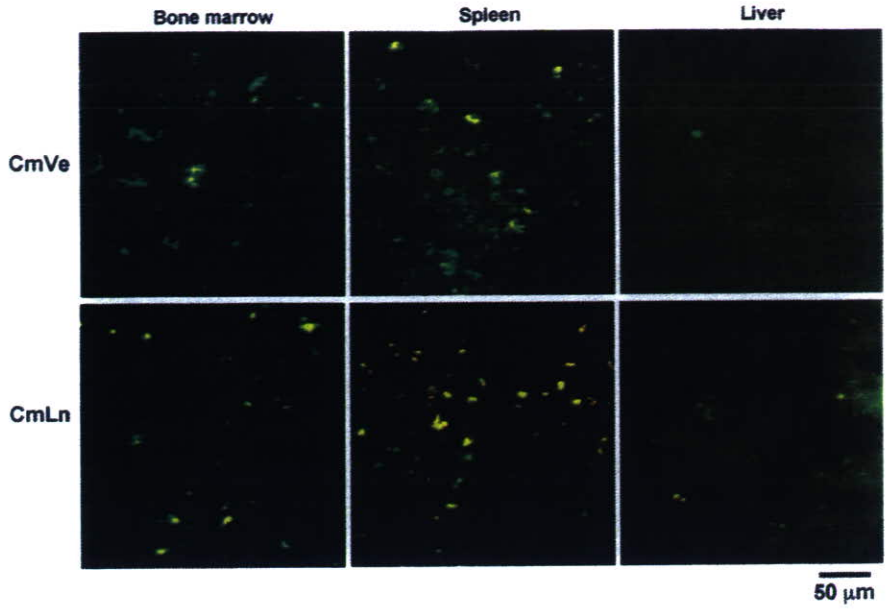

Fig. 7. Confocal scanning images of bone marrow, spleen, and liver collected from rat that received CmVe or CmLn dispersion (2 mg Cm/kg bw) 6 h after intravenous infusion. Yellow fluorescence indicates the distribution of Cm in organs.

4. Discussion

As Cm is a water-insoluble compound, Cm is conventionally administered orally, which has low bioavailability. The present study offered stable intravenous formulations using lipid-based nanoparticles. The binding constant for the interaction of Cm with egg and soy phosphatidylcholine was reported to be 3.26×10^5 and $2.64 \times 10^5\ M^{-1}$, respectively (Began et al., 1999), and that of phosphatidylcholine liposomes containing cholesterol was $2.5 \times 10^4\ M^{-1}$ (Kunwar et al., 2006). In our preliminary examination to determine the components of the bilayer membrane, vesicles that consisted of 1,2-dipalmitoyl-*sn*-glycero-3-phosphocholine and cholesterol (1/1, molar ratio) could solubilize much less Cm in bilayer membrane (below 3 wt.% of Cm to lipids) than DMPC vesicles, and the mixing examination of each component indicated that the low affinity of Cm to cholesterol causes the low solubilized capacity of bilayer membrane containing cholesterol (data not shown). Thus, we used DMPC without cholesterol to stably solubilize Cm. It has been reported that six molecules of phosphatidylcholine could bind one molecule of Cm (Began et al., 1999). As shown in Fig. 2, the maximum solubilization capacity of DMPC to Cm was determined to be approximately 10 wt.% and it was calculated that one Cm was fixed by 5.4 molecules of DMPC. These data are consistent with previous report (Began et al., 1999). In terms of preparation techniques, it should be considered that excess Cm formed solid precipitate which could be removed by filtration; however, as shown in Fig. 2, too much excess Cm decreased the solubilized amount of Cm. In the case of CmLn, the solubilization of Cm in employed oil was a factor for determining the maximum Cm content. Present soybean oil could solubilize Cm at approximately 10 mg mL^{-1} in preparation conditions.

Confocal scanning microscopic observation clearly indicated that Cm was solubilized in the bilayer membrane of vesicles or the inner oil phase of lipid-nanosphere in the present preparation procedure. TEM observation showed the oligolamellar membrane structure of CmVe (Fig. 3A). The spectroscopic analysis also indicated that the location of Cm is in the bilayer membrane (Fig. 4). In contrast, we could not find lamellar membrane structure in CmLn (Fig. 3B). ζ-potential measurement indicated that the carboxyl group of SA is located on the surface to characterize the surface with anion (Table 1). Thus, we identified two kinds of characterized anionic particles solubilizing Cm in their hydrophobic region as CmVe and CmLn. We have identified that surface modification of phospholipid vesicles with two compounds, SA and PEG-DSPE, cooperatively increases the distribution of vesicles into bone marrow macrophages (Sou et al., 2007).

As a therapeutic potential, CmVe showed scavenger ability against the ROS in several μM ranges (Fig. 5 and Table 2). It has been suggested that Cm is a potent agent for the suppression of septic or hemorrhagic organ failure (Lukita-Atmadja et al., 2002; Madan and Ghosh, 2003; Kaur et al., 2006; Siddiqui et al., 2006). Macrophages are target cells in such inflammation because they produce various mediators such as cytokines and ROS that promote inflammation following oxidative damage. Therefore, we were interested in the distribution of Cm in organs, in which the fluorescence of Cm was useful to detect the Cm in organs as shown in Fig. 7. At 6 h after injection, organ distribution of Cm in the present particulate system clearly indicated that the cellular components assumed to be macrophages are responsible for the uptake, especially in bone marrow and spleen. The competition of splenic uptake to bone marrow uptake would be more significant in rat model than that in previous pharmacokinetic study of vesicles containing SA in a rabbit model, because the rat spleen has about nine times larger capacity for uptake of vesicles compared with rabbit spleen (Sou et al., 2005, 2007). In liver, the relative high background fluorescence might

be due to the diffuse distribution of Cm. It is known that albumin can bind Cm when the binding constant is in the 10^4–10^5 M^{-1} range (Kunwar et al., 2006; Pulla Reddy et al., 1999: Barik et al., 2003). As this binding constant of albumin to Cm is equal to that of phospholipids, it is speculated that a fraction of Cm might be transferred from vesicles to serum albumin. The cellular uptake was not obvious in liver. Further pharmacokinetic study is necessary in order to determine the quantitative distribution of Cm in whole body. In present study, we indicated that the loading of Cm into tissue macrophages, mainly bone marrow and splenic macrophages, could be achieved in rats. In addition to the ROS scavenger ability, this system can be expected to efficiently suppress the NF-κB activation to inhibit the synthesis of iNOS in macrophages (Pan et al., 2000). These events should be a therapeutic benefit for treatment with oxidative injury and inflammation.

5. Conclusions

Two nanoparticles embedding Cm have been offered for intravenous injection of Cm. These nanoparticulate formulations could deliver Cm into tissue macrophages, specifically bone marrow and splenic macrophages in rats. This intravenous delivery system of Cm using lipid-based nanoparticles may be available for antioxidant and anti-inflammatory therapies.

Acknowledgements

This work was partly supported by the Japanese Ministry of Education, Culture, Sports, Science and Technology, through a Grant-in-Aid for Scientific Research (B) (17300162, 2005). The authors gratefully acknowledge Dr. William T. Phillips and Dr. Beth Goins (UTHSCSA) for suggestion and discussion for this research.

References

Barik, A., Priyadarsini, K.I., Mohan, H., 2003. Photophysical studies on binding of curcumin to bovine serum albumin. Photochem. Photobiol. 7, 597–603.

Began, G., Sudharshan, E., Udaya Sankar, K., Appu Rao, A.G., 1999. Interaction of curcumin with phosphatidylcholine: a spectrofluorimetric study. J. Agric. Food Chem. 47, 4992–4997.

Bruzell, E.M., Morisbak, E., Tønnesen, H.H., 2005. Studies on curcumin and curcuminoids. XXIX. Photoinduced cytotoxicity of curcumin in selected aqueous preparations. Photochem. Photobiol. Sci. 4, 523–530.

Chellat, F., Merhi, Y., Moreau, A., Yahia, L'H., 2005. Therapeutic potential of nanoparticulate systems for macrophage targeting. Biomaterials 26, 7260–7275.

Cheng, A.L., Hsu, C.H., Lin, J.K., Hsu, M.M., Ho, Y.F., Shen, T.S., Ko, J.Y., Lin, J.T., Lin, B.R., Ming-Shiang, W., Yu, H.S., Jee, S.H., Chen, G.S., Chen, T.M., Chen, C.A., Lai, M.K., Pu, Y.S., Pan, M.H., Wang, Y.J., Tsai, C.C., Hsieh, C.Y., 2001. Phase I clinical trial of curcumin, a chemopreventive agent, in patients with high-risk or pre-malignant lesions. Anticancer Res. 21, 2895–2900.

Kaur, G., Tirkey, N., Bharrhan, S., Chanana, V., Rishi, P., Chopra, K., 2006. Inhibition of oxidative stress and cytokine activity by curcumin in amelioration of endotoxin-induced experimental hepatoxicity in rodents. Clin. Exp. Immunol. 145, 313–321.

Kunchandy, E., Rao, M.N.A., 1990. Oxygen radical scavenging activity of curcumin. Int. J. Pharm. 58, 237–240.

Kunwar, A., Barik, A., Pandey, R., Priyadarsini, K.I., 2006. Transport of liposomal and albumin loaded curcumin to living cells: an absorption and fluorescence spectroscopic study. Biochim. Biophys. Acta. 1760, 1513–1520.

Kuo, M.L., Huang, T.S., Lin, J.K., 1996. Curcumin, an antioxidant and antitumor promoter, induces apoptosis in human leukemia cells. Biochem. Biophys. Acta. 1317, 95–100.

Li, L., Braiteh, F.S., Kurzrock, R., 2005. Liposome-encapsulated curcumin. In vitro and in vivo effects on proliferation, apoptosis, signaling, and angiogenesis. Cancer 104, 1322–1331.

Lukita-Atmadja, W., Ito, Y., Baker, G.L., McCuskey, R.S., 2002. Effect of curcuminoids as anti-inflammatory agents on the hepatic microvascular response to endotoxin. Shock 17, 399–403.

Madan, B., Ghosh, B., 2003. Diferuloylmethane inhibits neutrophil infiltration and improves survival of mice in high-dose endotoxin shock. Shock 19, 91–96.

Maiti, K., Mukherjee, K., Gantait, A., Saha, B.P., Mukherjee, P.K., 2007. Curcumin-phospholipid complex: preparation, therapeutic evaluation and pharmacokinetic study in rats. Int. J. Pharm. 330, 155–163.

Motterlini, R., Foresti, R., Bassi, R., Green, C.J., 2000. Curcumin, an antioxidant and anti-inflammatory agent, induces heme oxygenase-1 and protects endothelial cells against oxidative stress. Free Radic. Biol. Med. 28, 1303–1312.

Nishinaka, Y., Aramaki, Y., Yoshida, H., Masuya, H., Sugawara, T., Ichimori, Y., 1993. A new sensitive chemiluminescence probe, L-012, for measuring the production of superoxide anion by cells. Biochem. Biophys. Res. Commun. 193, 554–559.

Pan, M.N., Lin-Shiau, S.Y., Lin, J.K., 2000. Comparative studies on the suppression of nitric oxide synthase by curcumin and its hydrogenated metabolites through down-regulation of IkappaB kinase and NFkappaB activation in macrophages. Biochem. Pharmacol. 60, 1665–1676.

Pownall, H.J., Morrisett, J.D., Gotto Jr, A.M., 1977. Composition-structure-function correlations in the binding of an apolipoprotein to phosphatidylcholine bilayer mixtures. J. Lipid Res. 18, 14–23.

Pulla Reddy, A.C., Sudharshan, E., Appu Rao, A.G., Lokesh, B.R., 1999. Interaction of curcumin with human serum albumin—a spectroscopic study. Lipids 34, 1025–1029.

Schmid, M.C., Varner, J.A., 2007. Myeloid cell trafficking and tumor angiogenesis. Cancer Lett. 250, 1–8.

Sharma, R.A., Euden, S.A., Platton, S.L., Cooke, D.N., Shafayat, A., Hewitt, H.R., Marczylo, T.H., Morgan, B., Hemingway, D., Plummer, S.M., Pirmohamed, M., Gescher, A.J., Steward, W.P., 2004. Phase I clinical trial of oral curcumin: biomarkers of systemic activity and compliance. Clin. Cancer Res. 10, 6847–6854.

Sharma, R.A., Gescher, A.J., Steward, W.P., 2005. Curcumin: the story so far. Eur. J. Cancer 41, 1955–1968.

Shishodia, S., Sethi, G., Aggarwal, B.B., 2005. Curcumin: getting back to the roots. Ann. N.Y. Acad. Sci. 1056, 206–217.

Siddiqui, A.M., Cui, X., Wu, R., Dong, W., Zhou, M., Hu, M., Simms, H.H., Wang, P., 2006. The anti-inflammatory effect of curcumin in an experimental model of sepsis is mediated by up-regulation of peroxisome proliferator-activated receptor-gamma. Crit. Care Med. 34, 1874–1882.

Singh, S., Aggarwal, B.B., 1995. Activation of transcription factor NF-kappa B is suppressed by curcumin (diferuloylmethane). J. Biol. Chem. 270, 24995–25000.

Sou, K., Goins, B., Takeoka, S., Tsuchida, E., Phillips, W.T., 2007. Selective uptake of surface-modified phospholipid vesicles by bone marrow macrophages in vivo. Biomaterials 28, 2655–2666.

Sou, K., Kilpper, R., Goins, B., Tsuchida, E., Phillips, W.T., 2005. Circulation kinetics and organ distribution of Hb-vesicles developed as a red blood cell substitute. J. Pharmacol. Exp. Ther. 312, 702–709.

Tønnesen, H.H., 2002. Solubility, chemical and photochemical stability of curcumin in surfactant solutions. Studies of curcumin and curcuminoids, XXVIII. Pharmazie 57, 820–824.

Zeisberger, S.M., Odermatt, B., Marty, C., Zehnder-Fjällman, A.H.M., Ballmer-Hofer, K., Schwendener, R.A., 2006. Clodronate-liposome-mediated depletion of tumour-associated macrophages: a new and highly effective antiangiogenic therapy approach. Br. J. Cancer 95, 272–281.

Review | Journal of INTERNAL MEDICINE

doi: 10.1111/j.1365-2796.2007.01893.x

Haemoglobin-vesicles as artificial oxygen carriers: present situation and future visions

● H. Sakai[1], K. Sou[1], H. Horinouchi[2], K. Kobayashi[2] & E. Tsuchida[1]

From the [1]Oxygen Infusion Project, Advanced Research Institute for Science and Engineering, Waseda University; and [2]Department of General Thoracic Surgery, School of Medicine, Keio University; Tokyo, Japan

Abstract. Sakai H, Sou K, Horinouchi H, Kobayashi K, Tsuchida E (Research Institute for Science and Engineering, Waseda University; and School of Medicine, Keio University; Tokyo, Japan). Haemoglobin-vesicles as artificial oxygen carriers: present situation and future visions (Review). *J Intern Med* 2008; **263**: 4–15.

During the long history of development of haemoglobin (Hb)-based O_2 carriers (HBOCs), many side effects of Hb molecules have become apparent. They imply the physiological importance of the cellular structure of red blood cells. Hb-vesicles (HbV) are artificial O_2 carriers that encapsulate concentrated Hb solution with a thin lipid membrane. We have overcome the intrinsic issues of the suspension of HbV as a molecular assembly, such as stability for storage and in blood circulation, blood compatibility and prompt degradation in the reticuloendothelial system. Animal tests clarified the efficacy of HbV as a transfusion alternative and the possibility for other clinical applications. The results of ongoing HbV research make us confident in advancing further development of HbV, with the expectation of its eventual realization.

Keywords: artificial oxygen carrier, biocompatibility, liposome, nanotechnology, polyethylene glycol.

Introduction

Since the discovery of blood type antigen by Landsteinter in 1900, allogeneic blood transfusion has developed into a routine clinical practice; it has contributed to human health and welfare. Infectious diseases such as hepatitis and HIV have become widespread social problems, but a strict virus test by nucleic acid amplification test (NAT) is extremely effective to detect trace presences of a virus to minimize infection (although it is available mainly in a few developed countries). Even so, NAT poses problems such as detection limits during a window period and limited species of viruses for testing. Emergence of new viruses (such as West Nile virus, avian influenza and Ebola) and a new type of pathogen, prions, also threaten humans throughout the world. The preservation period of donated red blood cells (RBCs) is limited to 3 weeks in Japan. Immunological responses (such as anaphylaxis and graft-versus-host disease), and contingencies of blood type incompatibility further limit the utility of blood products. To obviate or minimize homologous transfusion, the transfusion trigger has been reconsidered, and roughly reduced from 10 to 6–8 g dL^{-1}. Bloodless surgery and preoperational enhancement of erythropoiesis for storing autologous blood have become common. However, these epoch-making treatments are not always practical for all patients. Some developed countries with ageing populations are confronting a decreasing number of young donors and an increasing number of aged recipients. Prohibition of blood donation from people who have travelled certain countries during a specific period also exacerbates the blood shortage in Japan. On the other hand, in some developing countries, establishment of a safe blood donation system is difficult. Under such circumstances, research of blood substitutes has gathered great attention and has been developed worldwide [1–4]. In Japan, for example, the government has given strong support to development of blood

substitutes in the wake of two tragedies: infection, by AIDS, of haemophiliac patients who had received nonpasteurized plasma products and the Great Hanshin Earthquake disaster. The requisites for artificial oxygen carriers that we develop should be not only effectiveness for tissue oxygenation, but also the following:

1 No blood type antigen and no infection (no pathogens);
2 Stability for long-term storage (e.g. over 2 years) at room temperature for stockpiling for any emergency;
3 Low toxicity and prompt metabolism, even after massive infusion;
4 Physichochemical properties that are adjustable to resemble those of human blood and
5 Reasonable production expense and cost performance.
Realization of such an artificial oxygen carrier will revolutionize transfusion medicine.

Physiological significance of cellular structure

Physicochemical measurements of O_2-releasing behaviours have revealed that the cellular structure of RBCs might not be effective for facilitating O_2 releasing in comparison with a homogeneous haemoglobin (Hb) solution [5–7]. However, nature has selected this cellular structure through evolution. The reasons for Hb encapsulation in RBCs are: (i) a decrease in the high colloidal osmotic pressure of Hb; (ii) prevention of the removal of Hb from blood circulation and (iii) preservation of the chemical environment in cells, such as the concentration of phosphates (2,3-diphosphoglyceric acid (DPG), ATP, etc.) and other electrolytes. Moreover, during the long history of the development of Hb-based O_2 carriers (HBOCs), many side effects of Hb molecules have become apparent, such as the dissociation of tetrameric Hb subunits into two dimers ($\alpha_2\beta_2 \rightarrow 2\alpha\beta$) that might induce renal toxicity, and entrapment of gaseous messenger molecules (NO and CO) inducing vasoconstriction, hypertension, reduced blood flow and tissue oxygenation at microcirculatory levels [8, 9], neurological disturbances, and the malfunctioning of oesophageal motor function [10]. These side effects of Hb molecules imply the importance of the cellular structure (Fig. 1).

Pioneering work of Hb encapsulation to mimic the cellular structure of RBCs was performed by Chang in 1957 [1], who prepared microcapsules (5 μm) made of nylon, collodion, etc. Toyoda in 1965 [11] and the Kambara-Kimoto group [12] also covered Hb solutions with gelatine, gum Arabic, silicone, etc. Nevertheless, it was shown to be extremely difficult to regulate the particle size that was appropriate for blood flow in the capillaries and to obtain sufficient biocompatibility. After Bangham and Horne reported in 1964 that phospholipids assemble to form vesicles in aqueous media, and that they encapsulate water-soluble materials in their inner aqueous interior [13], it seemed reasonable to use such vesicles for Hb encapsulation. Djordjevich and Miller in 1977 prepared liposome-encapsulated Hb (LEH) composed of phospholipids, cholesterol, fatty acids, etc. [14]. In the US, Naval Research Laboratories showed remarkable progress of LEH [15].

However, some intrinsic issues of encapsulated Hbs remained, mainly related to molecular assembly and particle dispersion. What we call Hb-vesicles (HbV) with high-efficiency production processes and their improved properties, were established by Tsuchida's group [16–18] based on technologies of molecular assembly and precise analysis of pharmacological and physiological aspects (Fig. 2). The salient characteristics of HbV are the following:

1 Human Hb is purified completely via pasteurization at 60 °C and ultrafiltration; no viruses exist [19–21];
2 A concentrated Hb solution, nearly 35 g dL^{-1}, is encapsulated with a thin bilayer membrane [16–18];
3 A new synthetic lipid is used to prevent platelet (PLT) activation [22, 23];
4 PEG-modification guarantees long-term storage over 2 years at room temperature, blood compatibility and extended circulation half-life [24–30];

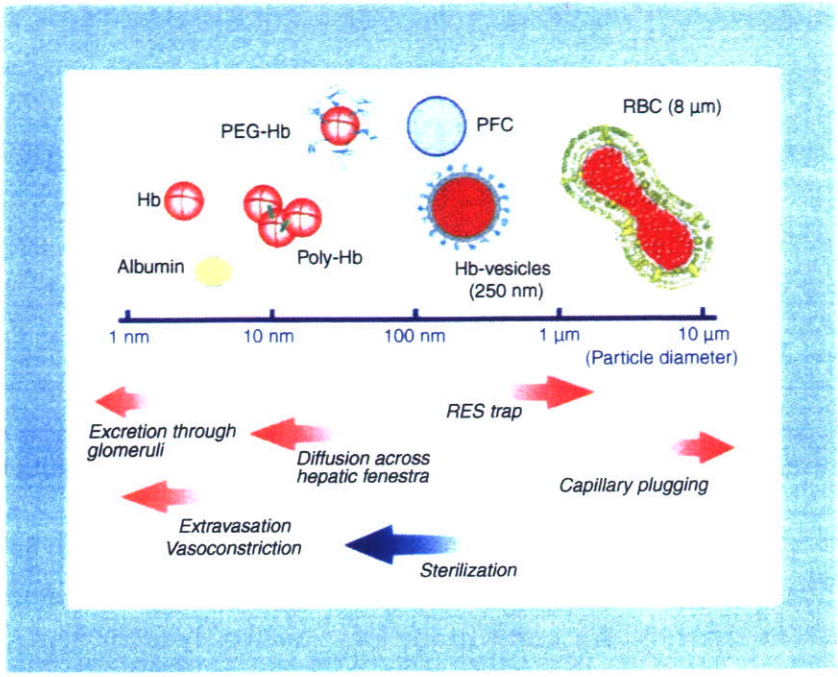

Fig. 1 What is the optimal dimension of artificial oxygen carriers? There is an upper limitation, below the capillary diameter, to prevent capillary plugging, and for the sterilization by membrane filters. On the other hand, the much smaller ones show higher rates of renal excretion and vascular wall permeabilities with side effects such as hypertension and neurological disturbances. Hb-vesicles show very low level of vascular wall permeabilities. Therefore, the Hb-vesicles seems appropriate from the viewpoint of hemodynamics. However, we have to clarify the influence of Hb-vesicles on the reticuloendothelial system (RES) because the fate of Hb-vesicles is RES trapping (see Fig. 3).

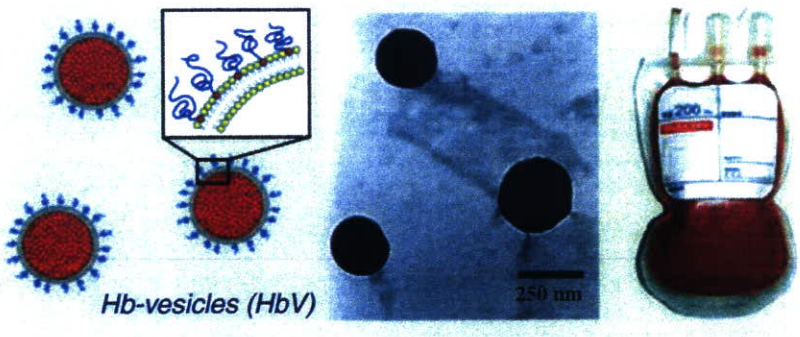

Fig. 2 (Left) Schematic representation of Hb-vesicle (HbV). One particle contains about 30 000 Hb molecules. The surface of one HbV is modified using polyethylene glycol chains that ensure the dispersion stability of HbV during storage and during circulation in the bloodstream. (Middle) The transmission electron micrograph depicts the well-regulated particle size (250 nm) and high Hb content within the vesicles. (Right) The packed HbV suspension looks turbid, like a mixture of milk and red wine, because of light-scattering of the particle suspension.

5 The cellular structure, which resembles that of RBCs, shields all side effects of Hb molecules, such as scavenging NO and CO [8, 9, 27];

6 The particle size (250 nm) is appropriate for sterilization, circulation persistence and biodistribution [18, 28] and

7 Hb-vesicles do not show colloid osmotic pressure. Addition of a plasma substitute solution such as recombinant albumin is effective to regulate colloid osmotic pressure [31–33].

Stabilized HbV for a long-term storage

Because Hb autoxidizes to form metHb and loses its O_2-binding ability during storage as well as during blood circulation, prevention of metHb formation is necessary. Some groups have reported a method to preserve deoxygenated Hbs in the liquid state [34] using well-known intrinsic characteristics of Hb: the Hb oxidation rate in a solution is dependent on the O_2 partial pressure; also, deoxyHb is not autoxidized at ambient temperatures [35]. For HbV, not only the inside Hb, but also the cellular structure (liposome) must be physically stabilized to prevent intervesicular aggregation, fusion and leakage of the encapsulated Hb.

Liposomes, as molecular assemblies, have been generally inferred to be structurally unstable. Many researchers have sought to develop stabilization methods that use polymer chains [36]. Polymerization of phospholipids that contain dienoyl groups was studied extensively in our group. For example, gamma-ray irradiation induces radiolysis of water molecules and generates OH radicals that initiate intermolecular polymerization of dienoyl groups in phospholipids. This method produces enormously stable liposomes, like rubber balls, which are resistant to freeze-thawing, freeze-drying and rehydration [37–39]. However, the polymerized liposomes were so stable that they were not degraded easily in the macrophages, even 30 days after injection [40]. It was concluded that polymerized lipids would not be appropriate for intravenous injection. Subsequently, it was clarified that selection of appropriate lipids (phospholipid/cholesterol/negatively charged lipid/PEG-lipid) and their composition are important to enhance the stability of liposomes without polymerization. Surface modification of liposomes with PEG chains is sufficient for dispersion stability [24–30].

We investigated the possibility of long-term preservation of HbV through a combination of two techniques, e.g. deoxygenation and PEG modification during storage for 2 years [24]. The PEG chains on the vesicular surface stabilize the dispersion state and prevent aggregation and fusion for 2 years because of their steric hindrance. The original metHb content (approximately 3%) before preservation decreased gradually to <1% in all samples after 1 month because of the presence of a reductant, such as homocysteine, inside the vesicles that consumed the residual O_2 and gradually reduced the trace amount of metHb. The rate of metHb formation was strongly dependent on the O_2 partial pressure: no increase in the metHb formation was observed because of the intrinsic stability of the deoxygenated Hb. In fact, the metHb content did not increase for 2 years. These results clearly indicate the possibility that the HbV suspension can be stored at room temperature for at least 2 years, which would enable stockpiling of HbV for any emergency.

Blood compatibility of Hb-vesicles

Liposome is not a solute but a particle in a suspension. Once injected, the surface is sometimes recognized by, or interacted with blood components. The so-called 'injection reaction', or pseudo-allergy is caused by complement activation with liposomal products [41] and a perfluorocarbon emulsion. Therefore, examination of blood compatibility of liposomal particles is important for clinical use. Transient thrombocytopenia in relation to complement activation is an extremely important haematological effect observed in rodent models after infusion of LEH (containing DPPG: 1,2-dipalmitoyl-*sn*-glycero-3-phosphatidyl glycerol), developed by the Naval Research Laboratory [42, 43]. In our group, exchange transfusion with the old-type HbV (containing DPPG, no PEG modification) in anesthetized rats resulted in thrombocytopenia [31]. Similar effects were also observed for administration of negatively charged liposomes [44, 45]. The transient reduction in PLT counts caused by liposomes was also associated with sequestration of PLTs in the lung and liver. Such non-physiological PLT activation would engender initiation and modulation of inflammatory responses because PLTs contain an array of potent proinflammatory

substance. However, the present HbV apparently does not induce thrombocytopenia in animal experiments, probably because the present HbV contains PEG-modification and a different type of negatively charged lipid (DHSG: 1,5-*O*-dihexadecyl-*N*-succinyl-L-glutamate), not DPPG or a fatty acid [22, 23].

Detailed blood compatibility of HbV in relation to negatively charged lipid was examined by Dr H. Ikeda at Hokkaido Red Cross Blood Center (Sapporo) and his colleagues [22, 23, 25, 46]. The present PEG-modified HbV containing DHSG did not affect the extrinsic or intrinsic coagulation activities of human plasma, whereas HbV containing DPPG and no PEG modification tended to shorten the intrinsic coagulation time. The kallikrein-kinin cascade of the plasma was activated slightly by DPPG-HbV, but not by the present PEG-DHSG-HbV. Moreover, the complement consumption of the plasma was observed by incubation with DPPG-HbV, but not with the present PEG-DHSG-HbV. These results indicate that the present PEG-DHSG-HbV has a higher biocompatibility with human plasma. Moreover, the exposure of human PLTs to high concentrations of the present HbV (up to 40%) *in vitro* did not cause PLT activation and did not adversely affect the formation and secretion of prothrombotic substances or proinflammatory substances that are triggered by PLT agonists. These results imply that HbV, at concentrations of up to 40%, has no aberrant interactions with either unstimulated or agonist-induced PLTs.

Biodistribution and fate of Hb-vesicles in reticuloendothelial system

The dose rate of blood substitutes would be considerably larger than those of other drugs, and their circulation time would be considerably shorter than RBC. Therefore, their biodistribution, metabolism, excretion and side effects must be characterized in detail especially about the reticuloendothelial system (RES).

Normally, free Hb released from RBC is bound rapidly to haptoglobin and is consequently removed from circulation by hepatocytes. However, when the Hb concentration is greater than the haptoglobin-binding capacity, unbound Hb is filtered through the kidney, where it is actively absorbed. Haemoglobinuria and eventual renal failure occur when the reabsorption capacity of the kidney is exceeded. The encapsulation of Hb in vesicles completely suppresses renal excretion. However, HbV in the bloodstream is ultimately captured by phagocytes in the RES (or mononuclear phagocytic system) in much the same manner as senescent RBC are, as confirmed by radioisotope ^{99m}Tc-labelled HbV injection [15, 28]. Gamma camera images of ^{99m}Tc-HbV showed that HbV remains in the bloodstream immediately after infusion so that the heart and liver that contain much blood showed strong intensity (Fig. 3a). However, HbV are finally distributed mainly in the liver, spleen and bone marrow. The circulation half-life is dose dependent; when the dose rate was 14 mL kg^{-1}, the circulation half-life was 32 h. The circulation time in the case of the human body can be estimated as twice or three times longer; or about 2 or 3 days at the same dose rate.

The time course of liver uptake was monitored using a confocal fluorescence microscope after fluorescence-labelled HbV was infused intravenously in an anesthetized hamster. Even though the individual particles of HbV were indistinguishable, they are recognizable with strong fluorescence when HbV are accumulated in phagosomes of Kupffer cells (Fig. 3b). Transmission electron microscopy (TEM) of the spleen 1 day after infusion of HbV clearly demonstrated the presence of HbV particles in macrophages, where HbV particles that appear as black dots are captured by the phagosomes [47] (Fig. 3c). However, after 7 days, the HbV structure cannot be observed. We confirmed transient splenomegaly with no irreversible damage to the organs and complete metabolism within a week. Immunochemical staining with a polyclonal anti-human Hb antibody was used as the marker of Hb in the HbV, and clarified that HbV almost disappeared after 7 days in both the spleen and liver (Fig. 3d) [47].

During metabolism of Hb, bilirubin and iron would be released. However, in our animal experiments of topload infusion, daily repeated infusions, and 40% blood exchange, neither of those products increased

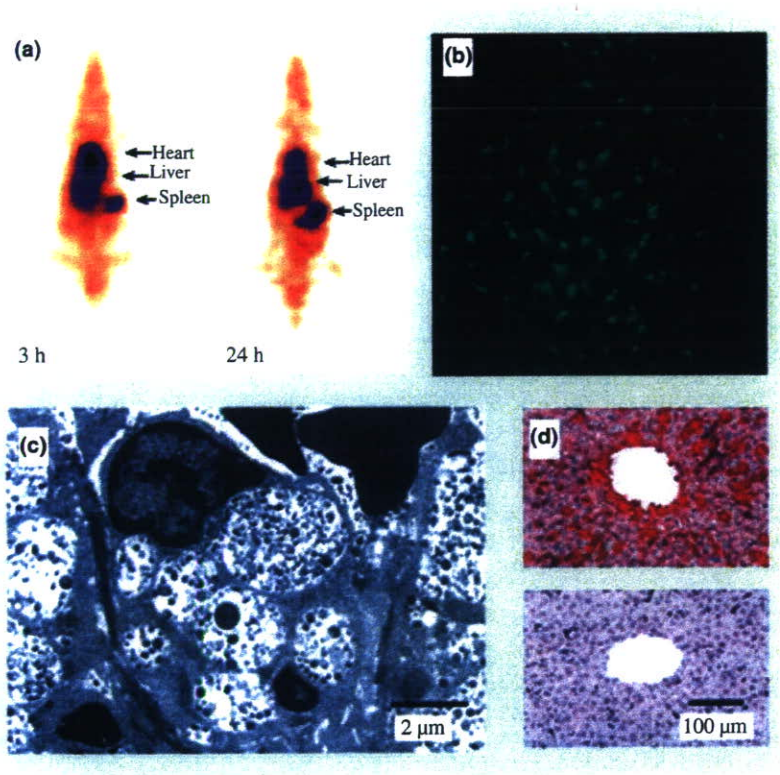

Fig. 3 Biodistribution and fate of Hb-vesicle (HbV). (a) Gamma-camera images of the distribution of ^{99m}Tc-labelled HbV in rats. At 3 h after injection, the heart and the liver showed a strong intensity because of the large blood volume. However, 24 h later, the intensity increased in the liver and spleen, the so-called reticuloendothelial system. (b) The liver surface of an anesthetized golden hamster 40 min after injection of fluorescence-labelled HbV observed using laser confocal scanning microscopy. The individual HbV particles flowing in the sinusoid are not detected, but the strong fluorescence is observed only in the Kupffer cells when they phagocyte HbV. (c) Transmission electron micrograph of rat spleen 1 day after intravenous injection of HbV. The small black dots are HbV near red blood cell in the capillaries and in the phagosomes of spleen macrophages. They disappear completely within 1 week. (d) Staining with anti-human Hb antibody revealed the presence of HbV in the liver Kupffer cells and sinusoids 1 day after infusion. However, they disappear within 1 week.

in the plasma within 14 days [33, 48, 49]. The released haeme from Hb in HbV might be metabolized by the inducible form of haeme oxygenase-1 in the Kupffer cells of the liver and the spleen macrophages. Bilirubin would normally be excreted in the bile as a normal pathway, and no obstruction or stasis of the bile should occur in the biliary tree. Berlin blue staining revealed considerable deposition of haemosiderin in the liver and spleen, even after 14 days. Normally, iron from a haeme is stored in the ferritin molecule. Both ferritin and haemosiderin release iron. They are anticipated to induce hydroxyl radical production followed by lipid peroxidation. The iron release rate from haemosiderin, however, is substantially less than that from ferritin. Consequently, the excess amount of iron would then normally be stored in an insoluble and less toxic form as haemosiderin. Hemosiderosis often occurs in patients who have received repeated blood transfusions because of the shorter half-life of the stored RBCs. Moderate splenomegaly and haemosiderin deposition were also confirmed in the spleen after injection of stored RBCs, partly because of the accumulation and degradation of stored RBCs with the lowered membrane deformability and shortened circulation half-life [33, 50].

As for the membrane components of HbVs, it was reported that the infused lipid components of

liposomes are entrapped in the Kupffer cells, and that phospholipid is metabolized and reused as a component of the cell membrane, or excreted in bile, especially as fatty acids and CO_2 in exhaled air. It was recently clarified using a ^{3}H-cholesterol that cholesterol of HbV is released from macrophages to blood, and is ultimately excreted in faeces. The PEG chain is widely used for surface modification of liposomal products. The chemical crosslinker of PEG-lipid is susceptible to hydrolysis to release PEG chains during metabolism. The released PEG chains, which are known as inert macromolecules, should be excreted in urine through the kidneys [51].

More precise data are necessary. However, these results imply that the metabolism of HbV and the excretion are within the physiological capacity that has been well characterized for the metabolism of senescent RBCs and conventional liposomal products.

Rheological properties and efficacy of an Hb-vesicle suspension as a transfusion alternative

A single HbV particle (approximately 250 nm diameter) contains about 30 000 Hb molecules. The HbV is much smaller than RBC, PLT or white blood cell (WBC) particles (Fig. 4a). Nevertheless, HbV acts as a particle in the blood and not as a solute; the colloid osmotic pressure of the HbV suspension is nearly zero. Addition of a plasma expander is necessary for a large substitution of blood to maintain the blood volume. The plasma expander candidates are human serum albumin (HSA), hydroxyethyl starch, dextran or gelatine, depending on the clinical setting, cost, country and clinician. Recombinant human serum albumin (rHSA) is an alternative [32, 33]. The impossibility of transmission of any infectious disease from humans is the greatest advantage of rHSA, which will soon be approved for clinical use in Japan [52].

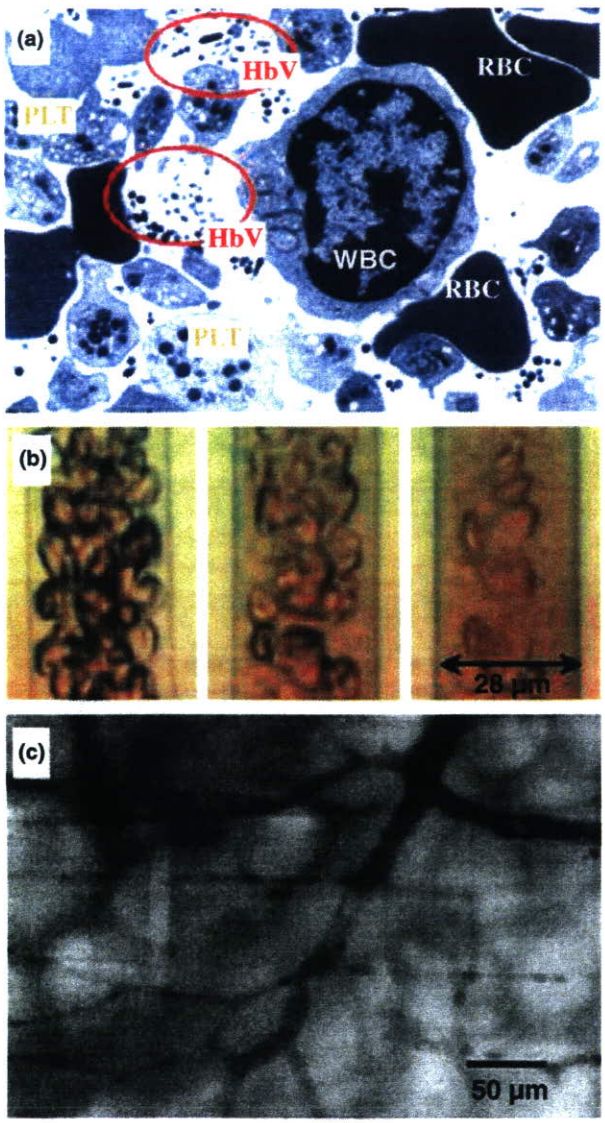

Fig. 4 How small is Hb-vesicle (HbV)? (a) The transmittance electron micrograph of rat blood 1 day after infusion of HbV. The buffy coat, obtained by a centrifugation of blood, was fixed using a 2.5% glutaraldehyde solution. Many HbV particles are visible in the red circles. They are much smaller than red blood cell (RBC), WBCs or PLT. (b) Flow patterns of the mixture of HbV and RBC suspended in recombinant human serum albumin in a narrow tube (centerline flow velocity: 1 mm s^{-1}). From left to right, the mixing ratios, RBC/HbV by volume are 100/0, 50/50 and 10/90 at a constant (Hb) = 10 g dL^{-1}. The RBCs tend to flow in the centerline, whereas HbV particles are dispersed homogeneously in a suspension medium. (c) Micrograph of a hamster skin microvasculature after 80% exchange transfusion with HbV suspended in 5% HSA solution, with an illumination with a wavelength of about 420 nm, being absorbed at the *Soret* band of Hb in HbV and RBC. The capillaries are blackened because of the homogeneous dispersion of HbV in the plasma phase. This homogeneous distribution believed to be effective for tissue oxygenation.

The rheological property of an artificial oxygen carrier is important because the infusion amount should be considerably large, which might affect the blood viscosity and hemodynamics. The viscosity of HbV suspended in 5%-rHSA was similar with that of blood, and the mixtures with RBC at various mixing ratios showed viscosities of 3–4 cP [53]. The main component to determine blood viscosity is RBC; the results indicate no great interaction between HbV and RBC. To observe the flow pattern of the mixture of HbV and RBC, they were mixed in various volume ratios. Then the suspension was perfused through an O_2-permeable narrow tube (28 μm inner diameter) and exposed to a deoxygenated environment [6]. Because HbV was dispersed homogeneously in the rHSA solution, increasing the volume of the HbV suspension thickened the marginal RBC-free layer and the plasma phase became semitransparent (Fig. 4b). The measurement of the O_2-release rate showed that HbV releases O_2 similarly to RBCs. On the other hand, an acellular Hb solution, in a comparative study, showed the facilitated O_2-release attributable to the effect of diffusion of small HbO_2. The slow O_2-release rate of HbV, which resembles that of RBC, is important to prevent autoregulatory vasoconstriction. Microvascular observation after 80% exchange transfusion with HbV suspended in HSA in conscious hamsters with a dorsal skin-fold window model of Prof. Intaglietta (UCSD) also showed that HbV was distributed homogeneously in the plasma phase; the capillary shape was visualized (Fig. 4c). This homogeneous distribution is inferred to be effective for improved blood flow and homogeneous tissue oxygenation.

Extensive *in vivo* studies of such HbV suspended in plasma-derived HSA or rHSA revealed sufficient O_2 transporting efficiency that is apparently comparable to RBCs in extreme blood exchange experiments [29–31, 33, 54–56] and fluid resuscitation from hemorrhagic shock [32, 57–60]. It was confirmed in rat models that haematopoietic activity was preserved and the decreased haematocrit returned to the original level within 1 or 2 weeks, whilst HbV captured in RES disappeared completely [33]. A recent experiment of HbV suspended in rHSA as a priming solution for cardiopulmonary bypass (CPB) in a rat model showed that HbV protects neurocognitive function by transporting O_2 to brain tissue even when the haematocrit is reduced markedly [61]. Homologous blood use is considered to be the gold standard for CPB priming in infants despite exposure of patients to potential cellular and humoral antigens. However, the results indicate that the use of HbV for CPB priming might prevent neurocognitive decline in infants because of considerable hemodilution. Other studies investigating HbV suspension as a possible perfusate for organ transplantation are also underway for the heart, liver, intestine, etc.

New concepts to design HbV

Development of artificial O_2 carriers was initiated originally with a simple idea and an expectation that the materials that bind or dissolve O_2 can behave similarly to RBCs in the bloodstream. Unfortunately, it was not so simple. During its long history of development, unexpected side effects were clarified such as capillary plugging, renal toxicity, vasoconstriction, vascular injury and accumulation. Decades-long R&D of artificial O_2 carriers has yielded no commercially available material for clinical use in Europe, Japan or the US. Recent advanced biotechnology enables *ex vivo* RBC production from haematopoietic stem cells [62]. However, problems remain of large-scale production and long-term storage for stockpiling. On the other hand, no doubts persist about the strong demand and expectation of a blood substitute.

The importance of the sophisticated function of RBCs in concert with vascular physiology has been clarified. New concepts are proposed in terms of the physicochemical properties of Hb-based artificial O_2 carriers. Historically, it has been regarded that the O_2 affinity is regulated similarly to RBCs (25–30 torr). Theoretically, this enables sufficient O_2 unloading during blood microcirculation, as can be evaluated according to the arterio-venous difference in O_2 saturation in accordance with an O_2 equilibrium curve. It has been expected that decreasing O_2 affinity (increasing P_{50}) increases O_2 unloading. However, this concept is controversial in light of recent findings because an excess O_2 supply would cause autoregulatory vasoconstriction